Journal of Computational Applied Mechanics 2023, 54(4): 552-576

DOI: 10.22059/JCAMECH.2023.360378.849

RESEARCH PAPER

Flexibility Matrix and Stiffness Matrix of 3D Curved Beam with Varying Curvature and Varying Cross-Sectional Area using Finite Displacement Transfer Method

Ashwinkumar G. Hansora [a], Harshvadan S. Patel [b,*]

[a] *Gujarat Technological University, Ahmedabad, Gujarat, 382424, India.*
[b] *Government Engineering College, Patan, affiliated to Gujarat Technological University, Ahmedabad, Gujarat, India.*

Abstract

Curved beams are widely used in combination with the linear elements of various civil engineering structures. Many researchers attempted to analyze beam curved in plan, beam curved in elevation, and spatial curved beam using different methods and different approaches and presented analytical exact solution and approximate numerical solution. The analytical exact integration of the governing differential equations is the major difficulty for the analysis of the geometrically non-linear curved beams. To overcome this difficulty, a finite displacement transfer method is proposed to eliminate analytical differentiation and integration, completely. This paper deals with the stiffness matrix of 3D curved beam with varying curvature and varying cross-sectional area. A novel finite displacement transfer method is used to determine displacements of the freely supported node of the cantilever 3D curved beam. The flexibility matrix is derived using the finite displacement transfer method. The stiffness matrix is derived by employing equilibrium and transformation matrix. The finite difference method is used for the numerical solution of the differential equations. Results of the calculation method are compared with the results of other methods in the literature and the FEM based analysis software. For the circular helix with uniformly varying cross-sectional area and 3600 elements, the maximum and minimum percentage difference in the stiffness coefficient is 2.89% and −0.65% respectively. For the elliptic helix with the uniform cross-sectional area and 720 elements, the maximum and minimum percentage difference in the stiffness coefficient is 2.69% and −2.65% respectively. The novel of this study lies in the generation of the stiffness matrix of the 3D curved beams without tedious analytical differentiation and integration of governing equations. The stiffness matrix of the spatial curved beam is applicable to the planer curved beam also.

Keywords: Rotation Matrix; Transformation Matrix; Internal Forces; Equilibrium Equations; Cartesian Coordinates.

1. Introduction

Curved beams have many applications in the field of civil engineering, such as curved stairs, curved

* Corresponding author. Harshvadan S. Patel, *E-mail address:* dr.hspatel@yahoo.com

balconies, curved bridges, etc. Sometimes the curved beams are used in the structure for the architectural purpose.

Majority of the civil engineering structures are statically indeterminate. In the statically indeterminate structure, the number of reactions or the number of internal forces exceed the number of static equilibrium equations. To evaluate unknown reactions and internal forces, compatibility equations are required in addition to equilibrium equations. In the analysis of indeterminate structure, it is necessary to satisfy the equilibrium equations, compatibility equations and force displacement equations. There are basically two distinct methods of analysis for statically indeterminate structure: Force method (Also known as flexibility method, method of consistent deformation) and Displacement method (Also known as stiffness method). In the flexibility method, first redundant are identified and removed to make the structure statically determinate. This structure is also known as released structure. The released structure is used for computation of displacements due to unit redundant [1]. Four different approaches of the force method of structural analysis are topological force methods, algebraic force methods, mixed algebraic-combinatorial force methods, and integrated force method [2-5]. The Integrated Force Method was proposed by Patnaik [6] for the analysis of discrete and continuous systems. Atluri et al. [1] assumed arbitrary cross-section of the curved beam but it is invariant along the axis of the curved beam. The analysis method proposed in the literature [2-7] increases size of the flexibility matrix as the number of elements increases. Finite difference method and Finite element method are some of the approximate methods of the analysis. Finite element method is most extensive. Accuracy of the result depends on the mesh refinement and higher order elements, but size of the problem also increases.

The curved beam can be analyzed applying Bernoulli–Euler and Timoshenko theories [8, 9]. The mechanical behaviour of the curved beam can be expressed by means of equilibrium equations, compatibility equations and constitutive relationships or by using energy principle [10-12]. The flexibility matrix and consequently the stiffness matrix of the curved beam can be obtained through force-displacement relationship derived from Castigliano's theorem. In any case, analytical solution requires integration of the governing equations. Hence, analytical solutions can be obtained for trivial shapes of the curved beam axis, such as circular and parabolic shapes [13-19]. In most of the cases, numerical methods must be employed for the solution of the governing equations of the curved beam [15-22]. To overcome difficulties in integration of the governing equations, many authors attempted different methods, such as differential quadrature method [23, 24].

R. Palaninathan [11] developed stiffness matrix of the circular 3D curved beam using Castigliano's theorem. Tore Dahlberg [12] investigated deflection of elliptical curved beam in plan using Castigliano's theorem in association with a MATLAB numerical integration algorithm and presented numerical solutions of the statically determinate and statically indeterminate problems. E. Marotta and P. Salvini [13] described plane curved beam geometry by polynomial function limited to cubic interpolation of the curvature radius and obtained stiffness matrix of the curved metal wire by inversion of analytical flexibility matrix (3×3) derived using Castigliano's theorem. E. Tufekci and O. Y. Dogruer [14] presented exact solution and derived fundamental matrix in terms of the reference coordinate for out-of-plane problem of an arch with varying curvature and cross-section. Analytical expressions of the fundamental matrix can be obtained only if the integral can be calculated analytically.

Gimena et. al. [15] presented structural behaviour of curved beam through twelve ordinary differential equations. Analytical solutions provided for the circular arch, circular balcony and helical beam defined in global coordinates. Dong Changjun [16] derived flexibility matrix of the variable curvature curved beam defined in polar coordinates using Castigliano's theorem. Flexibility coefficients and thereby obtained stiffness matrix for the curved beam axis equation $\rho=ae^{b\alpha}$ ($a>0$). Gimena et al. [15, 17-22] represented mechanical behaviour of the curved beam by a system of linear ordinary differential equations and developed transfer expression using Runge-Kutta method. The stiffness matrix was derived by rearranging the transfer equations [18, 19, 21]. Numerical procedure for the analysis of curved beam presented by Gimena et al. [21] requires parametric equations of flexion curvature and torsion curvature of the curved beam axis line.

Wankui Bu et al. [23] obtained partial differential governing equation of plane curved beam by theoretical analysis and presented finite difference scheme for governing equation, displacement component and stress component.

Chang-New Chen [24] presented finite element based solution of out-of-plane deflections of nonprismatic curved beam structures using differential quadrature element method (DQEM). Guodong Zhang et al. [25] presented formulation of finite elements and derived element stiffness matrix for arbitrary spatially curved 3-D beams using isogeometric approach. For the purpose of integration, the Guass quadrature rule is used.

Arici and Granata [26] developed a solution for space curved bar surrounded by a general wrinkler medium using the transfer matrix method. Yoda and Fuyama [27] attempted to examine validity of an analysis of thin-walled spatially curved beams approximated by an assemblage of straight curved beams. They concluded that the technique of an analysis of thin-walled spatially curved beams approximated by an assemblage of straight curved beams gives favorable results compared with analytically exact solution.

Other scholarly contributions to the theory of elasticity and applications to beams, plates, nanoring and nanoplates could be found in references.

Murin and Kutis [28] formulated stiffness matrix, nodal load vectors and beam transfer functions using finite element approach for arbitrary continuous smoothly cross-section varying 3D-beam element.

Sarria et al. [29] presented a formulation of curved beams with elastic supports. The stiffness matrix derived directly rearranging the transfer matrix. They presented a unique system of twenty four equations by joining the twelve equations of the stiffness matrix expression with the twelve equations of support conditions. Analytical method and numerical method (finite transfer method) implemented for the solution of the governing system of equations.

Michael N. Fardis et al. [30] constructed a stiffness matrix (12×12) of a free-standing helicoidal stair in terms of its geometric characteristics. Sundaramoorthy Rajasekaran and S. Padmanabhan [31] formulated curved beam equations using principle of virtual work. Yu Ai-min and Yi Ming [32] presented a theory for stresses and displacements of planer curved beam including warping. A. M. Yu et al. [33] derived differential equations of generalized warping coordinate for naturally curved and twisted beams with general cross-sectional shapes subjected to arbitrary load. Mohammad Rezaiee-Pajand and Niloofar Rajabzadeh-Safaei [34] suggested curved beam element with two nodes and six degrees of freedom to model parabolic members. Liping Liu and Nanshu Lu [35] presented a variational framework for large-displacement space curved beams. Weitong Guo et al. [36] developed an analytical displacement and internal force equations of curved beams considering vertical bending-torsion coupling. Mohammad Rezaiee-Pajand et al. [37] developed a curved beam element including First-order Shear Deformation Theory (FSDT) and the Green-Lagrange strain for geometrically nonlinear analysis of planar structures. Yi-Qun Tang et al. [38] presented geometrically nonlinear curved beam element based on the element-independent co-rotational (EICR) method. A. Borković et al. [39] presented geometrically exact nonlinear analysis of elastic in-plane beams in the context of finite but small strain theory. A. Borković et al. [40] developed geometrically exact Bernoulli–Euler beam using isogeometric approach.

Al-Azzawi AA [41] presented a finite difference equation by converting the governing differential equation of thin curved beams on frictional restraint Winkler foundation. Al-Azzawi et al. [42] presented finite differences equations of the governing differential equations for curved deep beams on elastic foundations represented by a Winkler model for frictional restraints. Cazzani et al. [43] analysed both straight and spatial Timoshenko beams using isogemetric approach, with particular emphasis on locking control. He et al. [44] derived generalized potential energy functional for curved beam with two kinds of variables and used B-spline wavelet on the interval (BSWI) as the interpolation function to construct the wavelet curved beam element. Pydah et al. [45] presented static analysis of bidirectional functionally graded circular beams considering smooth functional variations of the material properties along the beam axis and thickness simultaneously. Pietro et al. [46] investigated mechanical behaviour of three-dimensional curved beams through closed-form solution as well as one-dimensional finite elements based on Carrera's Unified Formulation.

Marotta et al. [47] presented finite element formulation of curved thin beams, useful for modelling structures made of filiform elements. They derived the stiffness matrix of the curved wire in closed form, through the application of Castigliano's Theorem. Horák et al. [48] extended the formulation of a 2D geometrically exact beam element proposed by Jirásek et al. [49] to curved elastic beams and approximated the first-order differential equations by the finite difference scheme and converted the boundary value problem to an initial value problem using the shooting method. Cammarata et el. [50] described direct kinetostatic analysis of a planar gripper with an elastic curved beam and calculated tangent stiffness matrix in closed form. Radenković and Borković [51] derived equilibrium and kinematic equations of an arbitrarily curved spatial Bernoulli-Euler beam with respect to a parametric coordinate; and stiffness matrix of an arbitrarily curved spatial beam using the flexibility approach.

Iandiorio and Salvini [52] presented an analytical solution for large planar displacements of cantilever beams, avoiding the integration of elliptic integrals. Magisano et al. [53] presented isogeometric weak formulations for large rotation analysis of shear deformable 3D beams and showed that coarse meshes with reduced number of unknowns gives accurate results compared to displacement-based isogeometric analysis and locking-free finite elements. Wu et al. [54] derived compliance matrix of general initially curved beams using Maxwell-Mohr Method under the collective framework of the polar coordinate system and Cartesian coordinate system. Nobaveh et al. [55] proposed adapting the endpoint stiffness of a spatially curved compliant beam using a movable torsional stiffener and a new graphical characterization method for the resulting anisotropic stiffness of the endpoint for large deflections.

Previous scholars employed different numerical methods for the solution of the governing differential equations [56, 57]; some of the scholars presented rigorous mathematical formulations for the analysis of circular, parabolic, elliptic, etc. curved beams which are almost difficult for the computer applications for the generalized spatial curved beam. Also, analysis methods suggested by previous scholars requires analytical differentiation, hence the methods are not generalized and needed formulation of problem specific differential equations. This gap is addressed in this study.

In this article, a general incremental finite displacement transfer method is proposed to obtain flexibility coefficients of the 3D curved beam. Stiffness matrix is derived using equilibrium conditions and transformation matrix. Finite difference method is used to evaluate the flexibility coefficients and stiffness coefficients of the spatial curved beam. The structural model presented in this article does not increase size of the stiffness matrix.

A comprehensive C++ computer program based on the calculation procedure presented in this article has been developed to obtain the values of the flexibility coefficients and stiffness coefficients. The numerical results have been compared with those found in the literature and with the values obtained using FEM based analysis software.The main practical application of the finite displacement transfer method for 3D curved beam is in the analysis and design of reinforced concrete spatial curved beam with bisymmetric cross-section. This method is useful when the geometry curved beam axis vary along the length of the curved beam.

2. Problem Statement

2.1 Practical Application of the Study

The curved beam is discretized to obtain flexibility matrix and stiffness matrix of the curved beam. Following assumptions have been made for the formulation of the finite displacement transfer method and verification of the method. (i) The material is elastic and homogeneous. (ii) The curved beam has two axes of symmetry in the cross section so that twisting moment and bending moment occurs independent of one another. (iii) Every cross-section remains rigid, i.e. undistorted, during deformation [56]. (iv) The length of the curved beam is large in comparison to the cross-sectional dimensions of the curved beam. (v) The interval $d\theta$ of the discretized elements is constant throughout length of the curved beam axis. (vi) Average values of the cross-sectional properties of discretized element are considered. These assumptions have been used throughout the study.

2.2 Difference between this Study and Previous Studies in the Literature

The major difference between this study and previous studies in the literature is that for the first time to the authors' knowledge, a rigorous, first principle approach is used to formulate the finite displacement transfer method; and this method is applied to derive flexibility matrix and stiffness matrix of any arbitrary 3D curved beams. The size of flexibility matrix 6×6 and size of stiffness matrix 12×12 remain unchanged, even if the curved beam discretized in to any number of elements. Cartesian coordinates of the curved beam axis, material properties and cross-sectional properties are sufficient to evaluate flexibility matrix and stiffness matrix of the curved beam; and no need to supply problem specific parametric equations of tangent, normal, binormal, flexion curvature or torsion curvature. The calculation method proposed in this study is applicable to the curved beam with any arbitrary geometrical axis and easy for the computer implementation.

2.3 Advantages of the Finite Displacement Transfer Method

- It makes possible to evaluate flexibility coefficients and stiffness coefficients without formulation of problem specific governing differential equations.
- This method eliminates analytical differentiation and integration of the equations.

- It is applicable to 3D curved beam with arbitrary geometrical axis and varying cross-sectional area.
- In this method the curved beam is divided in to several elements although size of the stiffness matrix remains 12×12.
- This method is easier for the user friendly computer application.

2.4 Disadvantages of the Finite Displacement Transfer Method

- The main disadvantage of the finite displacement transfer method is mandatory to supply Cartesian coordinates of the nodes of the curved beam axis as input data.
- It is required to supply the intervals of the discretized elements, if the interval is not uniform along the curved beam axis.

3. Fundamental Formulations

3.1 Geometry of the Curved Beam Axis

Figure 1 shows geometry of the curved beam axis with reference to right handed axis system *xyz*. Local axis (member axis) represented by *tnb* i.e. tangent, normal and binormal directions.

The Cartesian coordinates of the any node on the curved beam axis is $(x(\theta), y(\theta), z(\theta))$.

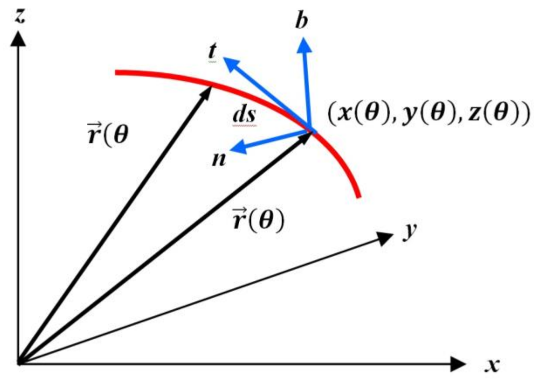

Figure 1: Geometry of the curved beam axis

The position vector can be given by,

$$\vec{r}(\theta) = x(\theta)I + y(\theta)J + z(\theta)K \tag{1}$$

where,

θ may be any independent variable

I, *J*, *K* are the unit vectors in the directions *x*, *y*, *z* respectively

Let, s and ds are the total arc length and elemental arc length of the curved beam axis respectively.

$$ds = \sqrt{(dx)^2 + (dy)^2 + (dz)^2} \tag{2}$$

Unit tangent,

$$T = T_1\, I + T_2\, J + T_3\, K \tag{3}$$

$$T_1 = dx/ds$$

$$T_2 = dy/ds$$

$$T_3 = dz/ds$$

Unit normal,

$$N = N_1\, I + N_2\, J + N_3\, K \tag{4}$$

$$N_1 = \frac{\left[(ds)^2 \cdot d(dx) - dx \cdot [dx \cdot d(dx) + dy \cdot d(dy) + dz \cdot d(dz)]\right]}{\begin{Bmatrix} \left[(ds)^2 \cdot d(dx) - dx \cdot [dx \cdot d(dx) + dy \cdot d(dy) + dz \cdot d(dz)]\right]^2 \\ + \left[(ds)^2 \cdot d(dy) - dy \cdot [dx \cdot d(dx) + dy \cdot d(dy) + dz \cdot d(dz)]\right]^2 \\ + \left[(ds)^2 \cdot d(dz) - dz \cdot [dx \cdot d(dx) + dy \cdot d(dy) + dz \cdot d(dz)]\right]^2 \end{Bmatrix}^{1/2}}$$

$$N_2 = \frac{\left[(ds)^2 \cdot d(dy) - dy \cdot [dx \cdot d(dx) + dy \cdot d(dy) + dz \cdot d(dz)]\right]}{\begin{Bmatrix} \left[(ds)^2 \cdot d(dx) - dx \cdot [dx \cdot d(dx) + dy \cdot d(dy) + dz \cdot d(dz)]\right]^2 \\ + \left[(ds)^2 \cdot d(dy) - dy \cdot [dx \cdot d(dx) + dy \cdot d(dy) + dz \cdot d(dz)]\right]^2 \\ + \left[(ds)^2 \cdot d(dz) - dz \cdot [dx \cdot d(dx) + dy \cdot d(dy) + dz \cdot d(dz)]\right]^2 \end{Bmatrix}^{1/2}}$$

$$N_3 = \frac{\left[(ds)^2 \cdot d(dz) - dz \cdot [dx \cdot d(dx) + dy \cdot d(dy) + dz \cdot d(dz)]\right]}{\begin{Bmatrix} \left[(ds)^2 \cdot d(dx) - dx \cdot [dx \cdot d(dx) + dy \cdot d(dy) + dz \cdot d(dz)]\right]^2 \\ + \left[(ds)^2 \cdot d(dy) - dy \cdot [dx \cdot d(dx) + dy \cdot d(dy) + dz \cdot d(dz)]\right]^2 \\ + \left[(ds)^2 \cdot d(dz) - dz \cdot [dx \cdot d(dx) + dy \cdot d(dy) + dz \cdot d(dz)]\right]^2 \end{Bmatrix}^{1/2}}$$

Unit binormal,

$$B = T \times N \tag{5}$$

$$B = B_1\, I + B_2\, J + B_3\, K \tag{6}$$

$$B_1 = (T_2 N_3 - T_3 N_2)$$

$$B_2 = (T_3 N_1 - T_1 N_3)$$

$$B_3 = (T_1 N_2 - T_2 N_1)$$

Rotation matrix,

$$[R] = \begin{bmatrix} T_1 & T_2 & T_3 \\ N_1 & N_2 & N_3 \\ B_1 & B_2 & B_3 \end{bmatrix} \tag{7}$$

Rotation matrix may be evaluated numerically as depicted in section 3.2.

3.2 Geometry of the Curved Beam Axis

The curved beam is discretized in to n number of segments as shown in figure 2. The interval dθ should be uniform throughout length of the curved beam.

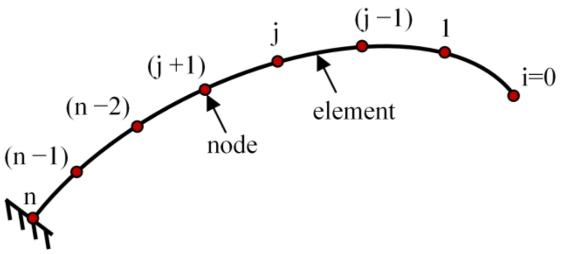

Figure 2: Descretization of the curved beam

$$x = x(\theta) = x_i \tag{8}$$

Introducing the centered difference formula,

$$dx = (x_{i+1} - x_{i-1})/2 \quad (9)$$

$$d^2x = d(dx) = x_{i+1} - 2x_i + x_{i-1} \quad (10)$$

Similarly,

$$y = y(\theta) = y_i \quad (11)$$

$$dy = (y_{i+1} - y_{i-1})/2 \quad (12)$$

$$d^2y = d(dy) = y_{i+1} - 2y_i + y_{i-1} \quad (13)$$

$$z = z(\theta) = z_i \quad (14)$$

$$dz = (z_{i+1} - z_{i-1})/2 \quad (15)$$

$$d^2z = d(dz) = z_{i+1} - 2z_i + z_{i-1} \quad (16)$$

Two imaginary nodes are considered for the above formulations i.e. one imaginary node before the node 0 and another after the node n.

4. Formulation of Flexibility Matrix

Concept of unit load method [56] is used to derive the flexibility matrix. A cantilever 3D curved beam is shown in figure 3. The node 0 is freely supported and node n is fixed.

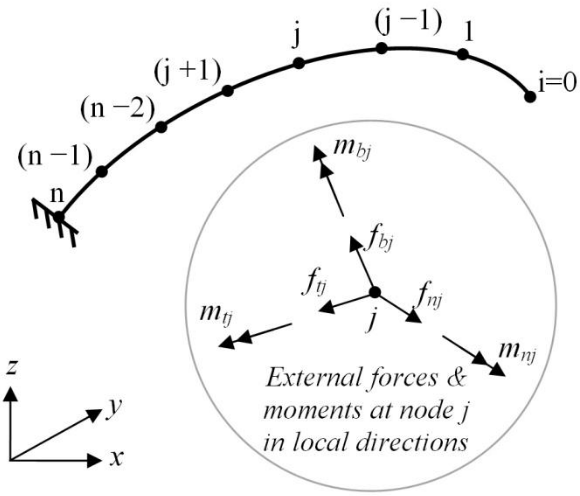

Figure 3: 3D Curved Cantilever Beam

Let, A is the cross-sectional area; E is the Young's modulus of elasticity; G is the shear modulus; I_t is the torsion constant; I_n and I_b are the moment of inertia; ξ_n and ξ_b are the shear coefficients.

The external forces and moments at node j in the local directions *tnb* are,

$$[f_{mj}] = [f_{tj} \quad f_{nj} \quad f_{bj}]^T \quad (17)$$

$$[m_{mj}] = [m_{tj} \quad m_{nj} \quad m_{bj}]^T \quad (18)$$

Also, the stress resultants (axial force, shear forces, twisting moment and bending moments) at node j in the local directions are,

$$[F_{mj}] = [F_{tj} \quad F_{nj} \quad F_{bj}]^T \quad (19)$$

$$[M_{mj}] = [M_{tj} \quad M_{nj} \quad M_{bj}]^T \quad (20)$$

The stress resultants can be obtained using the recursive scheme [26] as given below.

$$\begin{bmatrix} F_{mj} \\ M_{mj} \end{bmatrix} = \begin{bmatrix} f_{mj} \\ m_{mj} \end{bmatrix} + \begin{bmatrix} R_j & O \\ O & R_j \end{bmatrix} \begin{bmatrix} I & O \\ C_{j,(j-1)} & I \end{bmatrix} \begin{bmatrix} R^T_{(j-1)} & O \\ O & R^T_{(j-1)} \end{bmatrix} \begin{bmatrix} F_{m(j-1)} \\ M_{m(j-1)} \end{bmatrix} \tag{21}$$

where, $C_{j,(j-1)}$ is the coordinate transformation matrix [56] defined as

$$[C_{j,(j-1)}] = \begin{bmatrix} 0 & -(z_{(j-1)} - z_j) & (y_{(j-1)} - y_j) \\ (z_{(j-1)} - z_j) & 0 & -(x_{(j-1)} - x_j) \\ -(y_{(j-1)} - y_j) & (x_{(j-1)} - x_j) & 0 \end{bmatrix} \tag{22}$$

Now, for the jth element, the incremental finite deformations at the node j, relative to those at node j+1, produced by the stress resultants at node j in local directions can be obtained as follows [56]:

$$\begin{bmatrix} d\delta_{mj} \\ d\varphi_{mj} \end{bmatrix} = \begin{bmatrix} S_F & O \\ O & S_M \end{bmatrix} \begin{bmatrix} F_{mj} \\ M_{mj} \end{bmatrix} ds \tag{23}$$

where,

incremental finite displacements at node j in local directions,

$$[d\delta_{mj}] = [d\delta_{tj} \quad d\delta_{nj} \quad d\delta_{bj}]^T \tag{24}$$

incremental finite rotations at node j in local directions,

$$[d\varphi_{mj}] = [d\varphi_{tj} \quad d\varphi_{nj} \quad d\varphi_{bj}]^T \tag{25}$$

matrices of the elastic and geometrical properties,

$$[S_F] = \begin{bmatrix} 1/EA & 0 & 0 \\ 0 & \xi_n/GA & 0 \\ 0 & 0 & \xi_b/GA \end{bmatrix} \tag{26}$$

$$[S_M] = \begin{bmatrix} 1/GI_t & 0 & 0 \\ 0 & 1/EI_n & 0 \\ 0 & 0 & 1/EI_b \end{bmatrix} \tag{27}$$

The incremental finite deformations in global *xyz* directions can be obtained using following equation,

$$\begin{bmatrix} d\delta_{sj} \\ d\varphi_{sj} \end{bmatrix} = \begin{bmatrix} R^T_j & O \\ O & R^T_j \end{bmatrix} \begin{bmatrix} d\delta_{mj} \\ d\varphi_{mj} \end{bmatrix} \tag{28}$$

where,

incremental finite displacements at node j in global directions,

$$[d\delta_{sj}] = [d\delta_{xj} \quad d\delta_{yj} \quad d\delta_{zj}]^T \tag{29}$$

incremental finite rotations at node j in global directions,

$$[d\varphi_{sj}] = [d\varphi_{xj} \quad d\varphi_{yj} \quad d\varphi_{zj}]^T \tag{30}$$

The incremental finite deformations of the node j can be transformed to the node i in the global directions as given below [56]:

$$\begin{bmatrix} d\delta_{sji} \\ d\varphi_{sji} \end{bmatrix} = \begin{bmatrix} I & C_{ij} \\ O & I \end{bmatrix} \begin{bmatrix} d\delta_{sj} \\ d\varphi_{sj} \end{bmatrix} \tag{31}$$

where,

transformed finite displacements at node i in global directions,

$$[d\delta_{sji}] = [d\delta_{xji} \quad d\delta_{yji} \quad d\delta_{zji}]^T \tag{32}$$

transformed finite rotations at node i in global directions,

$$[d\varphi_{sji}] = [d\varphi_{xji} \quad d\varphi_{yji} \quad d\varphi_{zji}]^T \tag{33}$$

$$[C_{ij}] = \begin{bmatrix} 0 & (z_i - z_j) & -(y_i - y_j) \\ -(z_i - z_j) & 0 & (x_i - x_j) \\ (y_i - y_j) & -(x_i - x_j) & 0 \end{bmatrix}$$

It is noted that, $[C_{ij}] = -[C_{ji}]$

Cumulative transformed finite deformations is the total deformations of the node i in global directions.

$$\begin{bmatrix} \delta_{si} \\ \varphi_{si} \end{bmatrix} = \sum_{j=i}^{(n-1)} \begin{bmatrix} d\delta_{sji} \\ d\varphi_{sji} \end{bmatrix} \tag{34}$$

where,

$$[\delta_{si}] = [\delta_{xi} \quad \delta_{yi} \quad \delta_{zi}]^T \tag{35}$$

$$[\varphi_{si}] = [\varphi_{xi} \quad \varphi_{yi} \quad \varphi_{zi}]^T \tag{36}$$

The total deformations of the node i in local directions can be obtained as,

$$\begin{bmatrix} \delta_{mi} \\ \varphi_{mi} \end{bmatrix} = \begin{bmatrix} R_i & O \\ O & R_i \end{bmatrix} \begin{bmatrix} \delta_{si} \\ \varphi_{si} \end{bmatrix} \tag{37}$$

where,

$$[\delta_{mi}] = [\delta_{ti} \quad \delta_{ni} \quad \delta_{bi}]^T \tag{38}$$

$$[\varphi_{mi}] = [\varphi_{ti} \quad \varphi_{ni} \quad \varphi_{bi}]^T \tag{39}$$

To obtain flexibility coefficients, unit actions corresponding to f_{tj}, f_{nj}, f_{bj}, m_{tj}, m_{nj}, m_{bj} are applied one by one at node j (j=0). The deformations δ_{si}, φ_{si} (i=0) are the flexibility coefficients due to these unit actions.

Matrices of the unit actions are,

$$\begin{bmatrix} f_{tj=0} = 1 \\ f_{nj=0} = 0 \\ f_{bj=0} = 0 \\ m_{tj=0} = 0 \\ m_{nj=0} = 0 \\ m_{bj=0} = 0 \end{bmatrix}, \begin{bmatrix} f_{tj=0} = 0 \\ f_{nj=0} = 1 \\ f_{bj=0} = 0 \\ m_{tj=0} = 0 \\ m_{nj=0} = 0 \\ m_{bj=0} = 0 \end{bmatrix}, \begin{bmatrix} f_{tj=0} = 0 \\ f_{nj=0} = 0 \\ f_{bj=0} = 1 \\ m_{tj=0} = 0 \\ m_{nj=0} = 0 \\ m_{bj=0} = 0 \end{bmatrix}, \begin{bmatrix} f_{tj=0} = 0 \\ f_{nj=0} = 0 \\ f_{bj=0} = 0 \\ m_{tj=0} = 1 \\ m_{nj=0} = 0 \\ m_{bj=0} = 0 \end{bmatrix}, \begin{bmatrix} f_{tj=0} = 0 \\ f_{nj=0} = 0 \\ f_{bj=0} = 0 \\ m_{tj=0} = 0 \\ m_{nj=0} = 1 \\ m_{bj=0} = 0 \end{bmatrix}, \begin{bmatrix} f_{tj=0} = 0 \\ f_{nj=0} = 0 \\ f_{bj=0} = 0 \\ m_{tj=0} = 0 \\ m_{nj=0} = 0 \\ m_{bj=0} = 1 \end{bmatrix}$$

Flexibility coefficients can be evaluated numerically using equations (1) to (39).

Member flexibility matrix (6×6) corresponding to node 0 (i=0) is as follows,

$$[Fm]_{00} = \begin{bmatrix} \begin{bmatrix} \delta_{ti} \\ \delta_{ni} \\ \delta_{bi} \\ \varphi_{ti} \\ \varphi_{ni} \\ \varphi_{bi} \end{bmatrix}_{f_{tj=0}=1} & \begin{bmatrix} \delta_{ti} \\ \delta_{ni} \\ \delta_{bi} \\ \varphi_{ti} \\ \varphi_{ni} \\ \varphi_{bi} \end{bmatrix}_{f_{nj=0}=1} & \begin{bmatrix} \delta_{ti} \\ \delta_{ni} \\ \delta_{bi} \\ \varphi_{ti} \\ \varphi_{ni} \\ \varphi_{bi} \end{bmatrix}_{f_{bj=0}=1} & \begin{bmatrix} \delta_{ti} \\ \delta_{ni} \\ \delta_{bi} \\ \varphi_{ti} \\ \varphi_{ni} \\ \varphi_{bi} \end{bmatrix}_{m_{tj=0}=1} & \begin{bmatrix} \delta_{ti} \\ \delta_{ni} \\ \delta_{bi} \\ \varphi_{ti} \\ \varphi_{ni} \\ \varphi_{bi} \end{bmatrix}_{m_{nj=0}=1} & \begin{bmatrix} \delta_{ti} \\ \delta_{ni} \\ \delta_{bi} \\ \varphi_{ti} \\ \varphi_{ni} \\ \varphi_{bi} \end{bmatrix}_{m_{bj=0}=1} \end{bmatrix}$$

(40)

5. Formulation of Stiffness Matrix

Figure 4 shows the 3D curved beam fixed at both the ends. Properties of this curved beam are as mentioned in section 4.

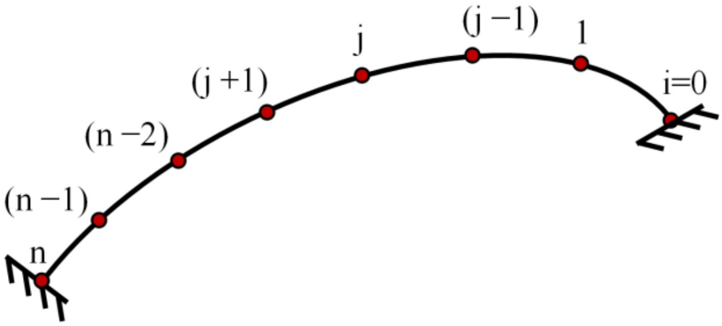

Figure 4: 3D curved beam fixed at both the ends

Stiffness matrix of the 3D curved beam can be obtained employing static equilibrium conditions as follows [56]. Stiffness matrix (12×12) in local directions,

$$[Km] = \begin{bmatrix} [Km]_{nn} & [Km]_{n0} \\ [Km]_{0n} & [Km]_{00} \end{bmatrix} \tag{41}$$

Stiffness matrix (12×12) in global directions,

$$[Ks] = \begin{bmatrix} [Ks]_{nn} & [Ks]_{n0} \\ [Ks]_{0n} & [Ks]_{00} \end{bmatrix} \tag{42}$$

$$[Km]_{00} = [Fm]_{00}^{-1} \tag{43}$$

$$[Ks]_{00} = [R_T]_0^T [Km]_{00} [R_T]_0 \tag{44}$$

where,

rotation transformation matrix, $[R_T]_0 = \begin{bmatrix} R_0 & O \\ O & R_0 \end{bmatrix}$

$$[Ks]_{n0} = -[Tr]_{n0} [Ks]_{00} \tag{45}$$

where,

transformation matrix, $[Tr]_{n0} = \begin{bmatrix} I & O \\ C_{n0} & I \end{bmatrix}$

$$[C_{n0}] = \begin{bmatrix} 0 & -(z_0 - z_n) & (y_0 - y_n) \\ (z_0 - z_n) & 0 & -(x_0 - x_n) \\ -(y_0 - y_n) & (x_0 - x_n) & 0 \end{bmatrix}$$

$$[Ks]_{0n} = [Ks]_{n0}^T \tag{46}$$

$$[Ks]_{nn} = -[Tr]_{n0} [Ks]_{0n} \tag{47}$$

Now, stiffness matrix in the local directions can be obtained as follows,

$$[Km] = \begin{bmatrix} [R_T]_n & [0] \\ [0] & [R_T]_0 \end{bmatrix} \begin{bmatrix} [Ks]_{n,n} & [Ks]_{n,0} \\ [Ks]_{0,n} & [Ks]_{0,0} \end{bmatrix} \begin{bmatrix} [R_T]_n^T & [0] \\ [0] & [R_T]_0^T \end{bmatrix} \tag{48}$$

$$[Km] = \begin{bmatrix} [R_T]_n[Ks]_{nn}[R_T]_n^T & [R_T]_n[Ks]_{n0}[R_T]_0^T \\ [R_T]_0[Ks]_{0n}[R_T]_n^T & [R_T]_0[Ks]_{00}[R_T]_0^T \end{bmatrix} \tag{49}$$

Equations 1 – 49 can be used to evaluate flexibility matrix and stiffness matrix numerically, without resorting to analytical differentiation and integration.

6. Verification of the Formulation

6.1 Circular helix with varying cross-sectional area

A circular helix with initial node 0 and final node n is shown in figure 5.

The circular helix has a radius 1m, a total angle π rad, and a height 3 m.

The cross-section is circular and linearly variable along the helix axis, with an initial diameter d_0 = 0.05 m and a final diameter d_n = 0.1 m.

The material of circular helix is same along the curve length, with modulus of elasticity E = 30 GPa and modulus of rigidity G = 12.5 GPa.

Shearing deformation is neglected.

Parametric equations of the helix axis are as follows,

$x = \cos\theta$

$y = \sin\theta$

$z = -3\theta/\pi$

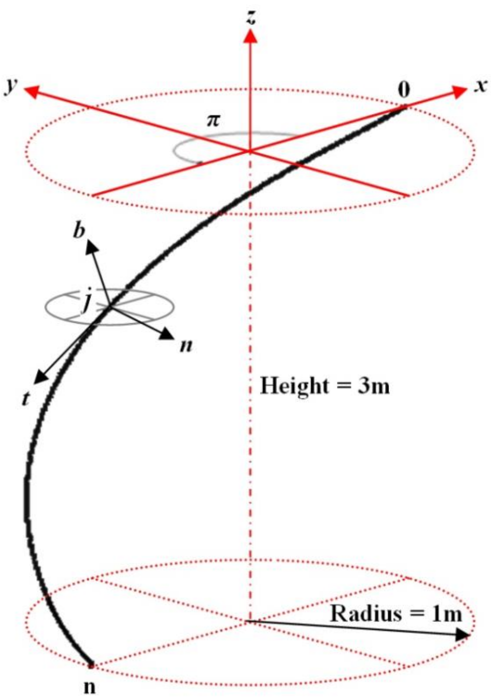

Figure 5: Circular helix with variable cross-section [**Error! Bookmark not defined.**]

Let, node 0 is freely supported and node n is fixed. The circular helix is discretized in to 3600 elements (interval dθ = π/3600). Unit actions are applied at the free end of the circular helix, one by one. The displacements at free end, obtained using equations (1) to (39) are compared (Figure 6) with the displacements obtained using FreeCAD software (version 0.18). FreeCAD .vkt file is used in the ParaView software (version 5.2.0) to get the numerical values of the displacements.

Table 1: Comparison of the displacements obtained from present study and results obtained from FreeCAD

Displacement	displacement due to unit force applied in tagential direction	displacement due to unit force applied in normal direction	displacement due to unit force applied in binormal direction	displacement due to unit moment applied about tagential direction	displacement due to unit moment applied about normal direction	displacement due to unit moment applied about binormal direction
δx (mm)*	7.727	-15.255	-3.581	1.958	-0.319	8.881
δx (mm)**	7.690	-15.193	-3.565	1.962	-0.313	8.931
δy (mm)*	8.128	-3.116	14.923	-2.747	7.500	3.022
δy (mm)**	8.100	-3.103	14.856	-2.750	7.531	3.030
δz (mm)*	-2.418	7.926	10.031	-2.807	4.958	-3.261
δz (mm)**	-2.410	7.892	9.983	-2.818	5.000	-3.275
% difference in δx	-0.48	-0.41	-0.45	0.16	-1.84	0.56
% difference in δy	-0.35	-0.41	-0.45	0.09	0.41	0.26
% difference in δz	-0.32	-0.43	-0.48	0.37	0.84	0.43

*Present Study, ** FreeCAD

Results shown in Table 1 indicate that the displacement values obtained from the present study and displacement values obtained from the FreeCAD is found to match. The unit action (force or moment) is applied in tangential / normal / binormal direction and displacements are measured with reference to positive x / y / z axis, hence value of displacement may be positive or negative. A negative value of the percentage difference indicates that the result obtained from present study is higher than the results obtained from the FreeCAD. A positive value of the percentage difference indicates that the result obtained from present study is lesser than the results obtained from the FreeCAD.

Now, the stiffness matrix [Km] evaluated by applying the calculation procedure described in this article with 3600 elements ($d\theta = \pi/3600$) is given below.

$$
[Km] = \begin{bmatrix}
329.34 & -333.85 & -371.80 & -166.14 & -310.64 & 119.73 & -356.23 & -333.85 & 346.13 & 79.87 & -254.88 & -150.71 \\
-333.85 & 634.61 & 594.17 & 150.92 & 717.50 & -681.87 & 578.15 & 634.61 & -360.87 & -19.05 & 210.79 & 340.70 \\
-371.80 & 594.17 & 793.98 & 495.45 & 1050.38 & -544.19 & 776.00 & 594.17 & -408.00 & -47.63 & 212.04 & 199.04 \\
-166.14 & 150.92 & 495.45 & 676.81 & 739.01 & -22.83 & 487.27 & 150.92 & -188.80 & -41.77 & 72.98 & 15.29 \\
-310.64 & 717.50 & 1050.38 & 739.01 & 1713.16 & -875.88 & 1034.95 & 717.50 & -358.72 & -1.59 & 210.90 & 195.26 \\
119.73 & -681.87 & -544.19 & -22.83 & -875.88 & 1207.21 & -538.09 & -681.87 & 144.68 & 14.81 & -8.16 & -415.00 \\
-356.23 & 578.15 & 776.00 & 487.27 & 1034.95 & -538.09 & 758.76 & 578.15 & -391.61 & -43.90 & 200.07 & 191.89 \\
-333.85 & 634.61 & 594.17 & 150.92 & 717.50 & -681.87 & 578.15 & 634.61 & -360.87 & -19.05 & 210.79 & 340.70 \\
346.13 & -360.87 & -408.00 & -188.80 & -358.72 & 144.68 & -391.61 & -360.87 & 364.56 & 81.98 & -264.38 & -159.73 \\
79.87 & -19.05 & -47.63 & -41.77 & -1.59 & 14.81 & -43.90 & -19.05 & 81.98 & 135.48 & -76.20 & 5.90 \\
-254.88 & 210.79 & 212.04 & 72.98 & 210.90 & -8.16 & 200.07 & 210.79 & -264.38 & -76.20 & 324.57 & 109.87 \\
-150.71 & 340.70 & 199.04 & 15.29 & 195.26 & -415.00 & 191.89 & 340.70 & -159.73 & 5.90 & 109.87 & 356.52
\end{bmatrix}
$$

Gimena et al. [19] presented following stiffness matrix using 1000 interval and fourth-order Runge-Kutta approximation.

$$[\mathrm{Km}] = \begin{bmatrix}
-329.55 & -334.05 & -371.89 & -166.09 & 310.66 & -119.83 & 356.3 & 334.06 & 346.34 & 79.95 & 255.17 & 150.95 \\
-334.05 & -634.75 & -594.10 & -150.79 & 717.21 & -681.83 & 578.07 & -634.77 & 361.08 & 19.11 & 211.09 & 341.04 \\
-371.89 & -594.10 & -793.62 & 495.07 & 1049.68 & 543.94 & 775.64 & -594.11 & 408.07 & 47.69 & 212.27 & 199.23 \\
-166.09 & -150.79 & 495.07 & -676.34 & 738.37 & -22.68 & 486.89 & -150.79 & 188.73 & 41.80 & 73.02 & 15.29 \\
310.66 & 717.21 & 1049.68 & 738.37 & -1711.83 & 875.28 & -1034.25 & 717.22 & -358.70 & -1.64 & -211.07 & 195.39 \\
-119.83 & -681.83 & 543.94 & -22.68 & 875.28 & -1206.91 & 537.84 & -681.84 & 144.78 & 14.80 & 8.31 & 415.26 \\
356.3 & 578.07 & 775.64 & 486.89 & -1034.25 & 537.84 & -758.39 & 578.09 & -391.67 & -43.95 & -200.28 & -192.07 \\
334.06 & -634.77 & -594.11 & -150.79 & 717.22 & -681.84 & 578.09 & -634.77 & 361.08 & 19.11 & 211.09 & 341.04 \\
346.34 & 361.08 & 408.07 & 188.73 & -358.7 & 144.78 & -391.67 & 361.08 & -364.78 & -82.07 & -264.68 & -159.97 \\
79.95 & 19.11 & 47.69 & 41.80 & -1.64 & 14.80 & -43.95 & 19.11 & -82.07 & -135.53 & -76.31 & 5.88 \\
255.17 & 211.09 & 212.27 & 73.02 & -211.07 & 8.31 & -200.28 & 211.09 & -264.68 & -76.31 & -324.91 & -110.11 \\
150.95 & 341.04 & 199.23 & 15.29 & 195.39 & 415.26 & -192.07 & 341.04 & -159.97 & 5.88 & -110.11 & -356.86
\end{bmatrix}$$

$$\%\ \mathrm{Diff.} = \begin{bmatrix}
0.06 & 0.06 & 0.02 & -0.03 & 0.01 & 0.08 & 0.02 & 0.06 & 0.06 & 0.10 & 0.11 & 0.16 \\
0.06 & 0.02 & -0.01 & -0.09 & -0.04 & -0.01 & -0.01 & 0.03 & 0.06 & 0.31 & 0.14 & 0.10 \\
0.02 & -0.01 & -0.05 & -0.08 & -0.07 & -0.05 & -0.05 & -0.01 & 0.02 & 0.13 & 0.11 & 0.10 \\
-0.03 & -0.09 & -0.08 & -0.07 & -0.09 & -0.66 & -0.08 & -0.09 & -0.04 & 0.07 & 0.05 & 0.00 \\
0.01 & -0.04 & -0.07 & -0.09 & -0.08 & -0.07 & -0.07 & -0.04 & -0.01 & 3.05 & 0.08 & 0.07 \\
0.08 & -0.01 & -0.05 & -0.66 & -0.07 & -0.02 & -0.05 & 0.00 & 0.07 & -0.07 & 1.81 & 0.06 \\
0.02 & -0.01 & -0.05 & -0.08 & -0.07 & -0.05 & -0.05 & -0.01 & 0.02 & 0.11 & 0.10 & 0.09 \\
0.06 & 0.03 & -0.01 & -0.09 & -0.04 & 0.00 & -0.01 & 0.03 & 0.06 & 0.31 & 0.14 & 0.10 \\
0.06 & 0.06 & 0.02 & -0.04 & -0.01 & 0.07 & 0.02 & 0.06 & 0.06 & 0.11 & 0.11 & 0.15 \\
0.10 & 0.31 & 0.13 & 0.07 & 3.05 & -0.07 & 0.11 & 0.31 & 0.11 & 0.04 & 0.14 & -0.34 \\
0.11 & 0.14 & 0.11 & 0.05 & 0.08 & 1.81 & 0.10 & 0.14 & 0.11 & 0.14 & 0.10 & 0.22 \\
0.16 & 0.10 & 0.10 & 0.00 & 0.07 & 0.06 & 0.09 & 0.10 & 0.15 & -0.34 & 0.22 & 0.10
\end{bmatrix}$$

Percentage difference in the stiffness coefficients as given above is calculated with reference to the stiffness coefficients presented by Gimena et al. [19]. To calculate percentage difference, appropriate change of sign (+/−) is taken in to account because axis, initial node and final node are different in present study and in the article of Gimena et al. [19].

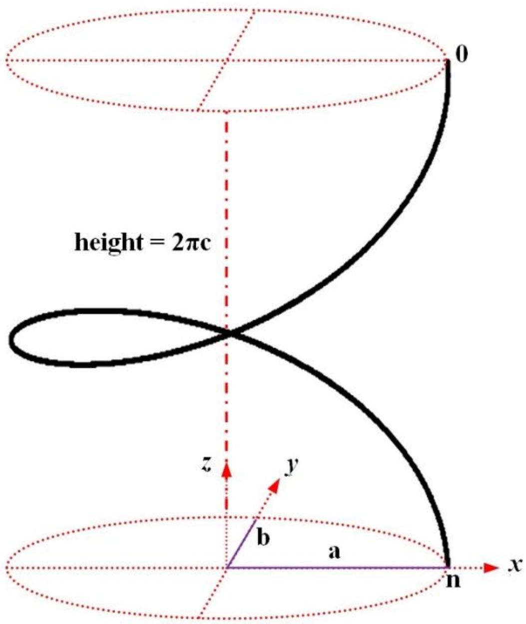

Figure 6: Elliptic–helical beam [21].

6.2 Elliptic–helical beam

An elliptic-helical beam with uniform cross-sectional area is shown in figure 6. Following data of the elliptic-helical beam [21] are used to obtain the stiffness matrix:

Semi-major axis, a = 4 ft; Semi-minor axis, b = 3 ft; Constant, c = 1.6 ft; Cross-sectional diameter=1 ft; Modulus of elasticity, E = 100000 kip/ft^2; Modulus of rigidity, G = 40000 kip/ft^2.

Shearing deformation is neglected.

Parametric equations of the elliptic-helical beam axis are as follows,

$$x = 4\cos\theta$$

$$y = 3\sin\theta$$

$$z = 1.6\,\theta$$

Let, node 0 ($\theta = 2\pi$) and node n ($\theta = 0$) are initial node and final node respectively, as shown in figure 7.

The stiffness matrix [Km] obtained when applying the calculation procedure described in this article with 720 elements ($d\theta = -\pi/360$) is as follows.

$$[Km] = \begin{bmatrix} 9.75 & 0.00 & -2.52 & -10.45 & -49.27 & -41.41 & -9.75 & 0.00 & 2.52 & 10.47 & -49.17 & 41.39 \\ 0.00 & 14.24 & 0.04 & 63.40 & 3.05 & -33.74 & 0.00 & -14.24 & -0.04 & 62.92 & -2.89 & -33.63 \\ -2.52 & 0.04 & 20.94 & 81.42 & 60.79 & 7.43 & 2.52 & -0.04 & -20.94 & -81.08 & 60.64 & -7.61 \\ -10.45 & 63.40 & 81.42 & 786.13 & 252.43 & -115.39 & 10.45 & -63.40 & -81.42 & -223.75 & 225.47 & -184.55 \\ -49.27 & 3.05 & 60.79 & 252.43 & 542.64 & 194.41 & 49.27 & -3.05 & -60.79 & -225.39 & 182.00 & -208.83 \\ -41.41 & -33.74 & 7.43 & -115.39 & 194.41 & 448.40 & 41.41 & 33.74 & -7.43 & -183.92 & 208.04 & -288.77 \\ -9.75 & 0.00 & 2.52 & 10.45 & 49.27 & 41.41 & 9.75 & 0.00 & -2.52 & -10.47 & 49.17 & -41.39 \\ 0.00 & -14.24 & -0.04 & -63.40 & -3.05 & 33.74 & 0.00 & 14.24 & 0.04 & -62.92 & 2.89 & 33.63 \\ 2.52 & -0.04 & -20.94 & -81.42 & -60.79 & -7.43 & -2.52 & 0.04 & 20.94 & 81.08 & -60.64 & 7.61 \\ 10.47 & 62.92 & -81.08 & -223.75 & -225.39 & -183.92 & -10.47 & -62.92 & 81.08 & 781.91 & -251.11 & -113.78 \\ -49.17 & -2.89 & 60.64 & 225.47 & 182.00 & 208.04 & 49.17 & 2.89 & -60.64 & -251.11 & 541.00 & -194.37 \\ 41.39 & -33.63 & -7.61 & -184.55 & -208.83 & -288.77 & -41.39 & 33.63 & 7.61 & -113.78 & -194.37 & 447.88 \end{bmatrix}$$

Gimena et al. [**Error! Bookmark not defined.**] presented following stiffness matrix using fourth-order Runge-Kutta approximation.

$$[Km] = \begin{bmatrix} -9.75 & 0 & 2.52 & 10.46 & -49.22 & 41.4 & 9.75 & 0 & -2.52 & -10.46 & -49.22 & -41.4 \\ 0 & -14.24 & 0 & 63.16 & -2.97 & -33.69 & 0 & 14.24 & 0 & 63.16 & 2.97 & -33.69 \\ 2.52 & 0 & -20.94 & -81.25 & 60.71 & -7.52 & -2.52 & 0 & 20.94 & 81.25 & 60.71 & 7.52 \\ 10.46 & 63.16 & -81.25 & -784.01 & 251.77 & 114.58 & -10.46 & -63.16 & 81.25 & 223.74 & 225.43 & 184.23 \\ -49.22 & -2.97 & 60.71 & 251.77 & -541.82 & 194.39 & 49.22 & 2.97 & -60.71 & -225.43 & -182 & -208.43 \\ 41.4 & -33.69 & -7.52 & 114.58 & 194.39 & -448.13 & -41.4 & 33.69 & 7.52 & 184.23 & 208.43 & 288.76 \\ 9.75 & 0 & -2.52 & -10.46 & 49.22 & -41.4 & -9.75 & 0 & 2.52 & 10.46 & 49.22 & 41.4 \\ 0 & 14.24 & 0 & -63.16 & 2.97 & 33.69 & 0 & -14.24 & 0 & -63.16 & -2.97 & 33.69 \\ -2.52 & 0 & 20.94 & 81.25 & -60.71 & 7.52 & 2.52 & 0 & -20.94 & -81.25 & -60.71 & -7.52 \\ -10.46 & 63.16 & 81.25 & 223.74 & -225.43 & 184.23 & 10.46 & -63.16 & -81.25 & -784.01 & -251.77 & 114.58 \\ -49.22 & 2.97 & 60.71 & 225.43 & -182 & 208.43 & 49.22 & -2.97 & -60.71 & -251.77 & -541.82 & -194.39 \\ -41.4 & -33.69 & 7.52 & 184.23 & -208.43 & 288.76 & 41.4 & 33.69 & -7.52 & 114.58 & -194.39 & -448.13 \end{bmatrix}$$

Percentage difference in the stiffness coefficients as given above is calculated with reference to the stiffness coefficients presented by Gimena et al. [21]. To calculate percentage difference, appropriate change of sign (+/−) is taken in to account because axis, initial node and final node are different in present study and in the article of Gimena et al. [21].

$$
\%\ \text{Diff.} = \left[\begin{array}{cccccccccccc}
0.00 & \text{---} & 0.00 & 0.10 & -0.10 & -0.02 & 0.00 & \text{---} & 0.00 & -0.10 & 0.10 & 0.02 \\
\text{---} & 0.00 & \text{---} & -0.38 & -2.69 & -0.15 & \text{---} & 0.00 & \text{---} & 0.38 & 2.69 & 0.18 \\
0.00 & \text{---} & 0.00 & -0.21 & -0.13 & 1.20 & 0.00 & \text{---} & 0.00 & 0.21 & 0.12 & -1.20 \\
0.10 & -0.38 & -0.21 & -0.27 & -0.26 & -0.71 & 0.10 & -0.38 & -0.21 & 0.00 & -0.02 & -0.17 \\
-0.10 & -2.69 & -0.13 & -0.26 & -0.15 & -0.01 & -0.10 & -2.69 & -0.13 & 0.02 & 0.00 & -0.19 \\
-0.02 & -0.15 & 1.20 & -0.71 & -0.01 & -0.06 & -0.02 & -0.15 & 1.20 & 0.17 & 0.19 & 0.00 \\
0.00 & \text{---} & 0.00 & 0.10 & -0.10 & -0.02 & 0.00 & \text{---} & 0.00 & -0.10 & 0.10 & 0.02 \\
\text{---} & 0.00 & \text{---} & -0.38 & -2.69 & -0.15 & \text{---} & 0.00 & \text{---} & 0.38 & 2.69 & 0.18 \\
0.00 & \text{---} & 0.00 & -0.21 & -0.13 & 1.20 & 0.00 & \text{---} & 0.00 & 0.21 & 0.12 & -1.20 \\
-0.10 & 0.38 & 0.21 & 0.00 & 0.02 & 0.17 & -0.10 & 0.38 & 0.21 & 0.27 & 0.26 & 0.70 \\
0.10 & 2.69 & 0.12 & -0.02 & 0.00 & 0.19 & 0.10 & 2.69 & 0.12 & 0.26 & 0.15 & 0.01 \\
0.02 & 0.18 & -1.20 & -0.17 & -0.19 & 0.00 & 0.02 & 0.18 & -1.20 & 0.70 & 0.01 & 0.06
\end{array}\right]
$$

7. Results and Discussion

In this section, stiffness coefficients in the member directions (*tnb*) of the 3D curved beam are obtained for the different interval and the results are compared with the results available in the literature. Circular helix with varying cross-sectional area and elliptic–helical beam with uniform cross-sectional area are considered for the comparison of the results. Later, flexibility matrix and stiffness matrix are obtained for the curved beam with varying geometry along its axis.

7.1 Circular helix with varying cross-sectional area

Stiffness coefficients of the circular helix with varying cross-sectional area and parameters as given in section .1; are determined for the intervals π/900 (900 elements), π/1800 (1800 elements) and π/3600 (3600 elements). The obtained results are compared and percentage difference is calculated with the results available in the research paper [19]. Figure 7 and figure 8 shows the comparison of the stiffness coefficients and percentage difference in the stiffness coefficients of the circular helix with varying cross-sectional area with reference to the research paper [19].

Comparison of the results (Figure 7 & 8) shows that the stiffness coefficients match with the stiffness coefficients available in the literature [**Error! Bookmark not defined.**]. In the case of 900 elements (interval $d\theta = \pi/900$), the maximum and minimum percentage difference in the stiffness coefficient is 11.36% and −2.55% respectively. The average positive and negative percentage difference in the stiffness coefficients is 0.73% and 0.31% respectively. In the case of 1800 elements (interval $d\theta = \pi/1800$), the maximum and minimum percentage difference in the stiffness coefficient is 5.72% and −1.28% respectively. The average positive and negative percentage difference in the stiffness coefficients is 0.36% and 0.15% respectively. In the case of 3600 elements (interval $d\theta = \pi/3600$), the maximum and minimum percentage difference in the stiffness coefficient is 2.89% and −0.65% respectively. The average positive and negative percentage difference in the stiffness coefficients is 0.18% and 0.08% respectively. Figure 7 and figure 8 shows that the convergence rate is fast. The percentage difference in the results can be reduced to approximately half by doubling the elements.

7.2 Elliptic–helical beam with uniform cross-sectional area

Stiffness coefficients in the member directions (*tnb*) of the elliptic–helical beam with uniform cross-sectional area and parameters as given in section 5.2; are determined for the intervals π/90 (180 elements), π/180 (360 elements) and π/360 (720 elements). The obtained results are compared and percentage difference is calculated with the results available in the research paper [21]. Figure 9 and figure 10 shows the comparison of the stiffness coefficients and percentage difference in the stiffness coefficients of the elliptic–helical beam with uniform cross-sectional area with reference to the research paper [21].

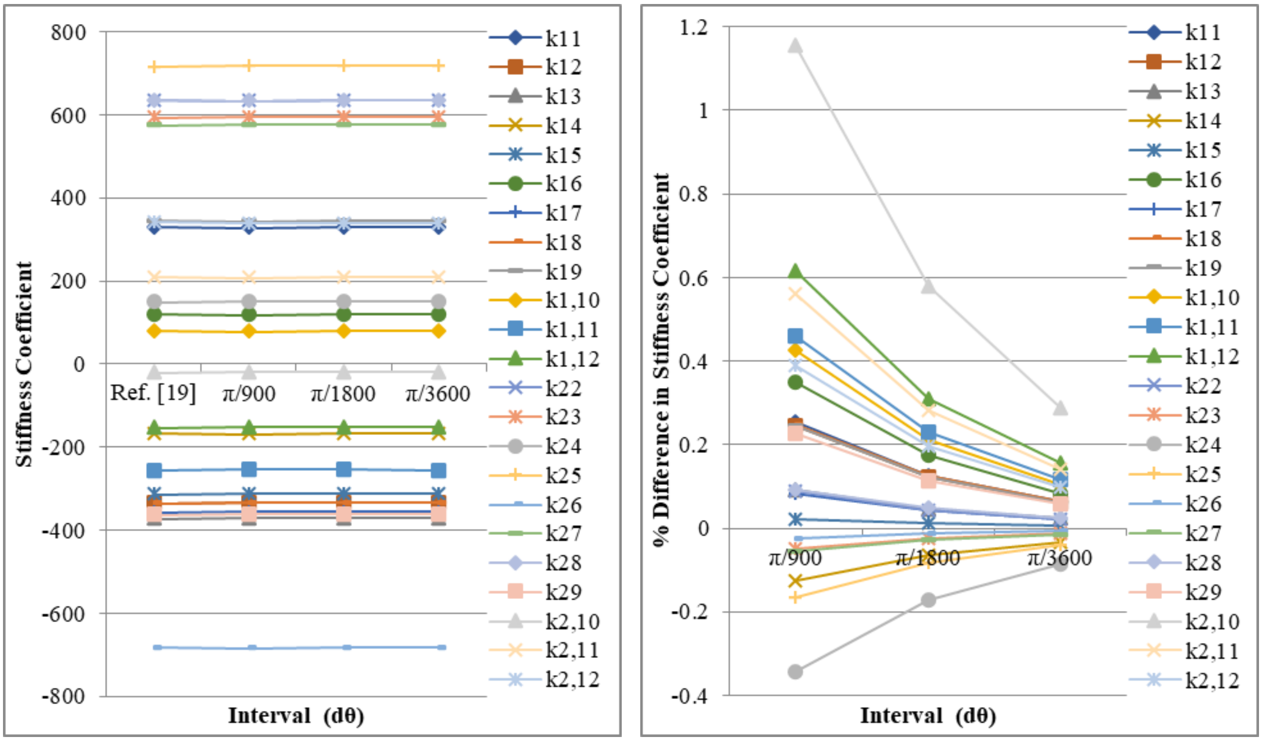

Figure 7: Comparison of stiffness coefficients (k11 to k2,12) for circular helix with varying cross-sectional area at different interval between present study and past study.

Comparison of the results (Figure 9 & 10) shows that the stiffness coefficients match with the stiffness coefficients available in the literature [21]. In the case of 180 elements (interval dθ = -π/90), the maximum and minimum percentage difference in the stiffness coefficient is 10.65% and −10.73% respectively. The average positive and negative percentage difference in the stiffness coefficients is 1.56% and 1.20% respectively. In the case of 360 elements (interval dθ = -π/180), the maximum and minimum percentage difference in the stiffness coefficient is 5.35% and −5.34% respectively. The average positive and negative percentage difference in the stiffness coefficients is 0.78% and 0.61% respectively. In the case of 720 elements (interval dθ = -π/360), the maximum and minimum percentage difference in the stiffness coefficient is 2.69% and −2.65% respectively. The average positive and negative percentage difference in the stiffness coefficients is 0.38% and 0.32% respectively. Figure 9 and figure 10 shows that the convergence rate is fast. The percentage difference in the results can be reduced to approximately half by doubling the elements.

7.3 Spatial (3D) Curved Beam with varying Geometry of Curved Beam Axis

2. Following parameters are considered to obtain flexibility matrix and stiffness matrix of the 3D curved beam with varying geometry of curved beam axis:

$$x = 5\cos\theta,\ y = 4\sin\theta,\ z = 1.5\,\theta \qquad 0 \le \theta \le \pi/2$$

$$x = 4\cos\theta,\ y = 4\sin\theta,\ z = 1.5\,\theta \qquad \pi/2 \le \theta \le \pi$$

$$x = 4\cos\theta,\ y = 3\sin\theta,\ z = 1.5\,\theta \qquad \pi \le \theta \le 3\pi/2$$

The cross-section is rectangular with a width b = 0.230 m and depth d=0.450 m. The material is same along the curve length, with modulus of elasticity E = 30 GPa and modulus of rigidity G = 12.5 GPa. Shearing deformation is neglected.

Let, node 0 is at θ = 0 and node n is at θ = 3π/2.

The flexibility matrix $[Fm]_{00}$ and stiffness matrix [Km] of the 3D curved beam with 540 elements (dθ = π/360) are given below.

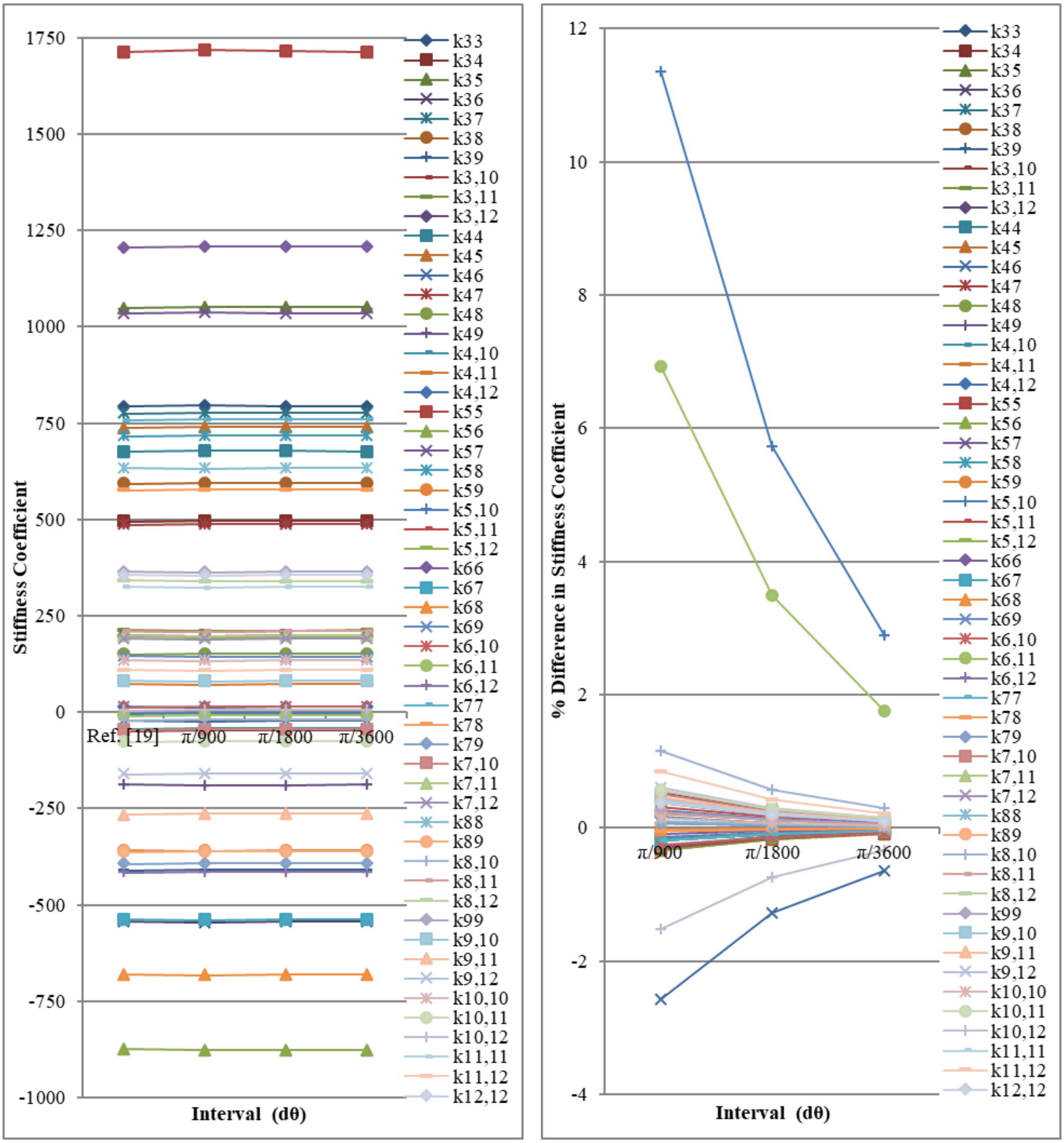

Figure 8: Comparison of stiffness coefficients (k33 to k12,12) for circular helix with varying cross-sectional area at different interval between present study and past study.

$$
[\bar{F}m]_{00} = 10^{3}\begin{bmatrix}
67.33 & -14.16 & -8.65 & 0.99 & -2.63 & 7.40 \\
-14.16 & 23.23 & -17.72 & 2.03 & 0.35 & -2.49 \\
-8.65 & -17.72 & 51.87 & -5.18 & 2.23 & -1.33 \\
0.99 & 2.03 & -5.18 & 0.90 & 0.09 & 0.22 \\
-2.63 & 0.35 & 2.23 & 0.09 & 0.90 & -0.05 \\
7.40 & -2.49 & -1.33 & 0.22 & -0.05 & 1.36
\end{bmatrix}
$$

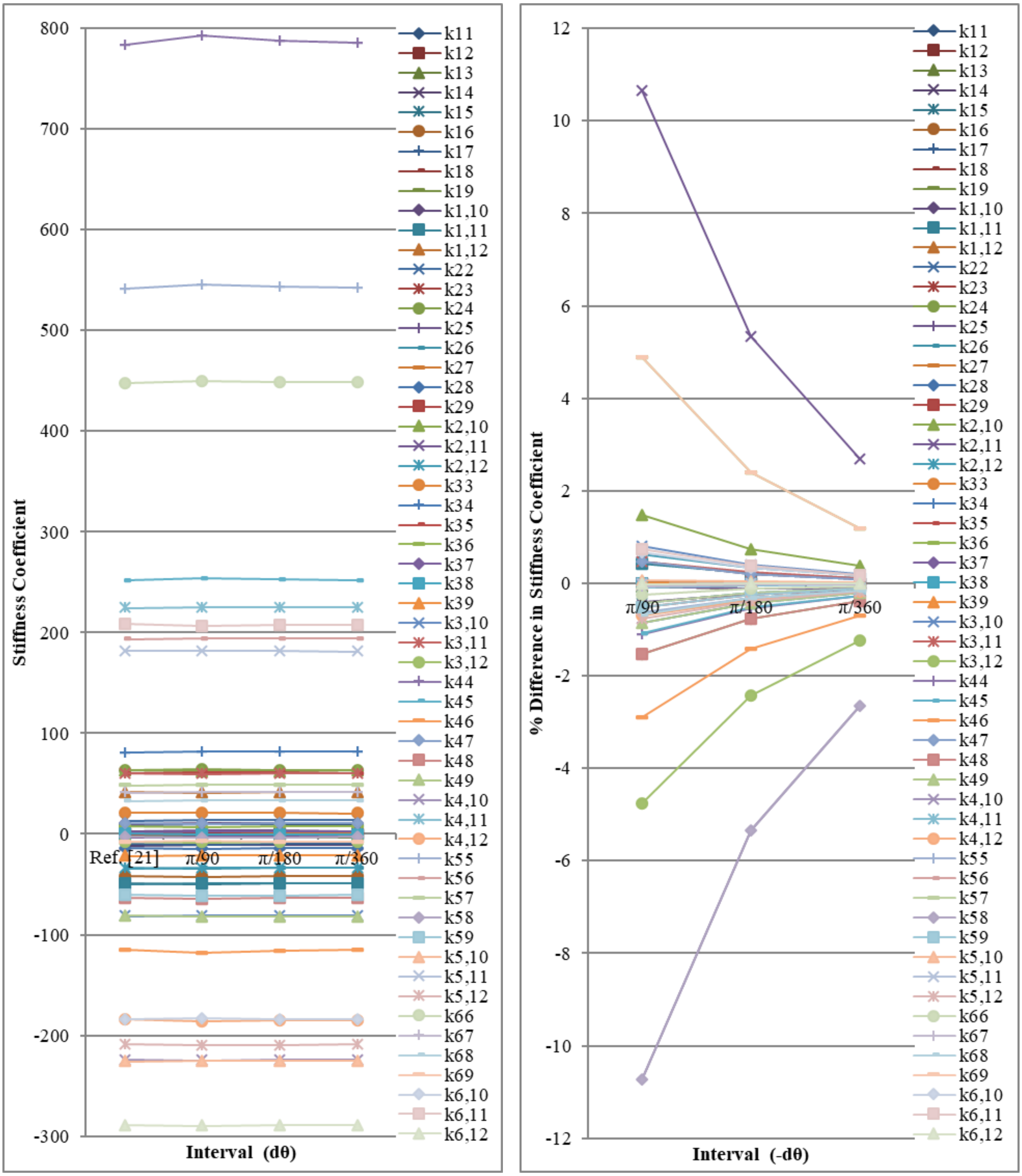

Figure 9: Comparison of stiffness coefficients (k11 to k6,12) for elliptic-helical beam with uniform cross-sectional area at different interval between present study and past study.

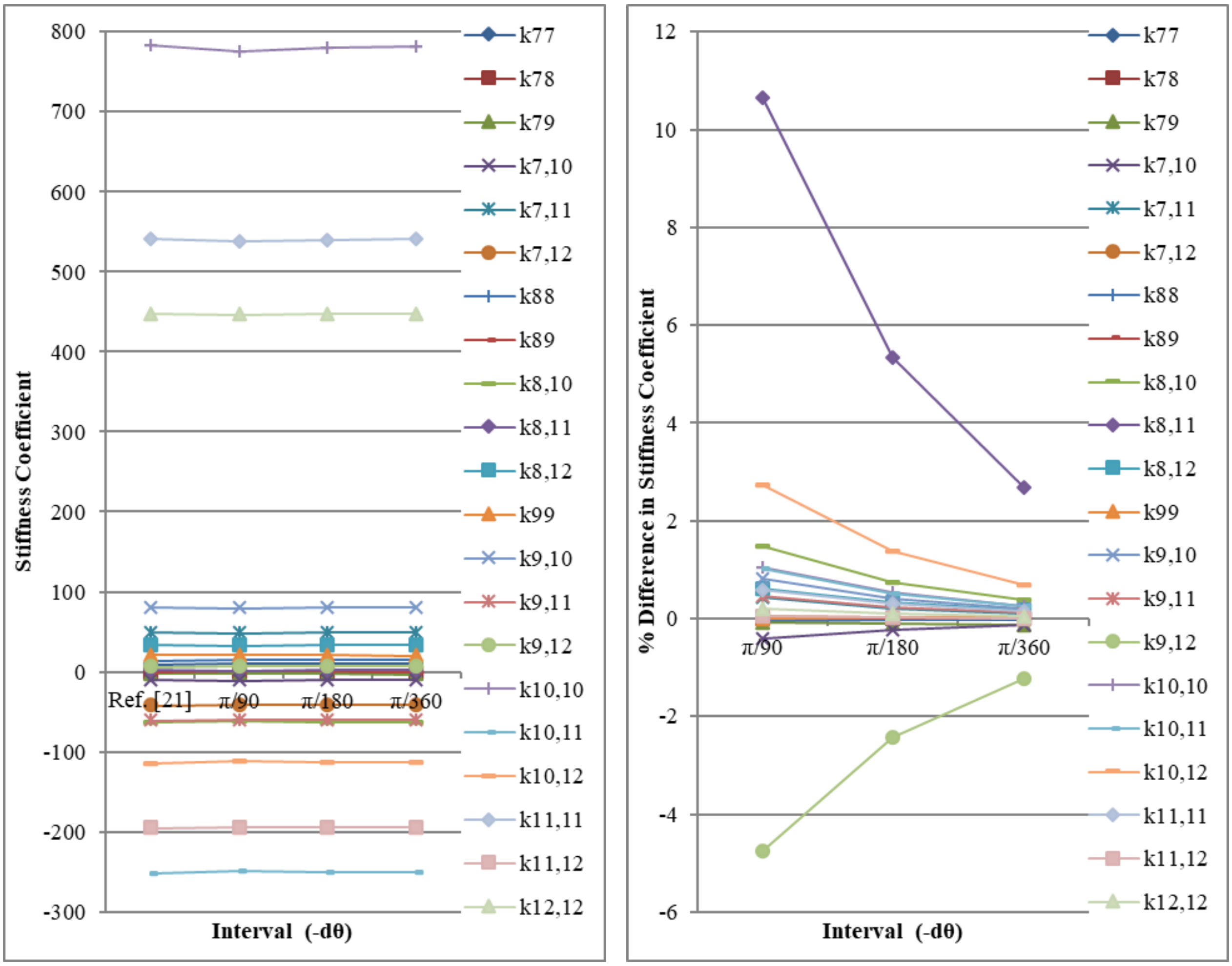

Figure 10: Comparison of stiffness coefficients (k77 to k12,12) for elliptic-helical beam with uniform cross-sectional area at different interval between present study and past study.

$$[Km] = \begin{bmatrix} 78.48 & 16.71 & -45.79 & -149.60 & -346.31 & -350.75 & -10.27 & 89.56 & 20.21 & -128.02 & -89.06 & 257.13 \\ 16.71 & 75.03 & -43.31 & 28.88 & -168.25 & -185.88 & -58.07 & 30.85 & 58.82 & 272.51 & -333.96 & 374.65 \\ -45.79 & -43.31 & 118.45 & 430.16 & 413.29 & 246.69 & 7.26 & -84.47 & -104.00 & -393.09 & 337.82 & -221.25 \\ -149.60 & 28.88 & 430.16 & 3216.65 & 1516.42 & 372.15 & -150.02 & -291.12 & -317.80 & -1294.37 & 1626.30 & -6.04 \\ -346.31 & -168.25 & 413.29 & 1516.42 & 3262.33 & 1612.77 & 64.36 & -469.37 & -307.55 & -1708.60 & 1246.76 & -935.30 \\ -350.75 & -185.88 & 246.69 & 372.15 & 1612.77 & 2494.63 & 136.19 & -415.03 & -166.22 & -23.15 & 462.98 & -2288.35 \\ -10.27 & -58.07 & 7.26 & -150.02 & 64.36 & 136.19 & 53.25 & -12.16 & -23.38 & -110.14 & 212.61 & -309.76 \\ 89.56 & 30.85 & -84.47 & -291.12 & -469.37 & -415.03 & -12.16 & 113.52 & 55.44 & 18.16 & -202.01 & 318.45 \\ 20.21 & 58.82 & -104.00 & -317.80 & -307.55 & -166.22 & -23.38 & 55.44 & 105.19 & 482.40 & -384.15 & 240.98 \\ -128.02 & 272.51 & -393.09 & -1294.37 & -1708.60 & -23.15 & -110.14 & 18.16 & 482.40 & 4039.70 & -1891.06 & 390.67 \\ -89.06 & -333.96 & 337.82 & 1626.30 & 1246.76 & 462.98 & 212.61 & -202.01 & -384.15 & -1891.06 & 2865.65 & -1499.77 \\ 257.13 & 374.65 & -221.25 & -6.04 & -935.30 & -2288.35 & -309.76 & 318.45 & 240.98 & 390.67 & -1499.77 & 3124.44 \end{bmatrix}$$

The flexibility matrix $[Fm]_{00}$ and stiffness matrix [Km] of the 3D curved beam with 1080 elements ($d\theta = \pi/720$) are given below.

$$[Fm]_{00} = 10^3 \begin{bmatrix} 67.44 & -14.17 & -8.70 & 0.99 & -2.63 & 7.41 \\ -14.17 & 23.26 & -17.70 & 2.03 & 0.35 & -2.49 \\ -8.70 & -17.70 & 51.86 & -5.17 & 2.23 & -1.34 \\ 0.99 & 2.03 & -5.17 & 0.90 & 0.09 & 0.22 \\ -2.63 & 0.35 & 2.23 & 0.09 & 0.90 & -0.05 \\ 7.41 & -2.49 & -1.34 & 0.22 & -0.05 & 1.36 \end{bmatrix}$$

$$[Km] = \begin{bmatrix} 78.37 & 16.70 & -45.62 & -148.90 & -345.21 & -350.33 & -10.30 & 89.40 & 20.10 & -128.59 & -88.85 & 257.14 \\ 16.70 & 75.12 & -43.40 & 28.49 & -168.54 & -186.17 & -58.13 & 30.87 & 58.93 & 273.30 & -334.63 & 375.21 \\ -45.62 & -43.40 & 118.36 & 429.60 & 412.65 & 246.27 & 7.35 & -84.27 & -104.01 & -393.79 & 338.13 & -221.43 \\ -148.90 & 28.49 & 429.60 & 3212.26 & 1513.53 & 369.56 & -149.56 & -290.26 & -317.68 & -1296.22 & 1626.69 & -5.94 \\ -345.21 & -168.54 & 412.65 & 1513.53 & 3259.13 & 1609.13 & 64.70 & -468.12 & -307.46 & -1713.18 & 1247.96 & -934.38 \\ -350.33 & -186.17 & 246.27 & 369.56 & 1609.13 & 2493.34 & 136.54 & -414.50 & -166.10 & -22.50 & 463.78 & -2289.60 \\ -10.30 & -58.13 & 7.35 & -149.56 & 64.70 & 136.54 & 53.28 & -12.22 & -23.47 & -110.58 & 213.11 & -310.23 \\ 89.40 & 30.87 & -84.27 & -290.26 & -468.12 & -414.50 & -12.22 & 113.29 & 55.33 & 17.87 & -201.92 & 318.52 \\ 20.10 & 58.93 & -104.01 & -317.68 & -307.46 & -166.10 & -23.47 & 55.33 & 105.27 & 483.48 & -384.73 & 241.34 \\ -128.59 & 273.30 & -393.79 & -1296.22 & -1713.18 & -22.50 & -110.58 & 17.87 & 483.48 & 4051.67 & -1896.03 & 391.40 \\ -88.85 & -334.63 & 338.13 & 1626.69 & 1247.96 & 463.78 & 213.11 & -201.92 & -384.73 & -1896.03 & 2869.40 & -1502.72 \\ 257.14 & 375.21 & -221.43 & -5.94 & -934.38 & -2289.60 & -310.23 & 318.52 & 241.34 & 391.40 & -1502.72 & 3128.15 \end{bmatrix}$$

Above practical application demonstrates that though the curved beam axis having different geometry in different segments, there is no need to formulate distinct system of equations for each part of the spatial curved beam.

8. Conclusion

In this article, the curved beam centroidal axis is expressed in terms of parametric equations. An incremental finite displacement transfer method is presented to determine the flexibility matrix and stiffness matrix of a geometrically nonlinear 3D structural curved beam with varying cross-sectional area. Following conclusions are drawn with reference to the method presented and results obtained.

- A novel finite displacement transfer method presented in this article eliminates problem specific mathematical formulation of governing equations.
- The flexibility matrix and stiffness matrix of the 3D curved beam can be evaluated numerically without resorting to tedious analytical differentiation and integration.
- Finite displacement transfer method does not require creating distinct set of governing equations, if geometry of the curved beam is different in different segments of the curved beam.
- The finite displacement transfer method is found to be rapidly convergent.
- Cartesian coordinates of the curved beam axis, material properties and cross-sectional properties are sufficient to evaluate flexibility matrix and stiffness matrix of the curved beam, provided that the interval dθ is uniform throughout the length of the curved beam axis; and no need to supply problem specific parametric equations of tangent, normal, binormal, flexion curvature or torsion curvature.

Notations / Nomenclature

3D	three-dimensional
2D	two-dimensional
$\vec{r}(\theta)$	position vector
θ	independent variable
$x(\theta), y(\theta), z(\theta)$	Cartesian coordinates
I, J, K	unit vectors in the directions x, y, z respectively
s	total arc length
ds	elemental arc length

$d\theta$	interval
dx, dy, dz	first derivative of $x(\theta)$, $y(\theta)$, $z(\theta)$ respectively
d^2x, d^2y, d^2z	second derivative of $x(\theta)$, $y(\theta)$, $z(\theta)$ respectively
t, n, b	tangential, normal and binormal directions respectively
T, N, B	unit tangent, unit normal and unit binormal respectively
T_1, T_2, T_3	resolved parts of unit tangent in the directions x, y, z respectively
N_1, N_2, N_3	resolved parts of unit normal in the directions x, y, z respectively
B_1, B_2, B_3	resolved parts of unit binormal in the directions x, y, z respectively
$[R]$	rotation matrix (3×3)
$[R_i]$	rotation matrix of the node i (3×3)
x_i, y_i, z_i	Cartesian coordinates of the node i
A	cross-sectional area
$[f_{mj}]$	matrix of external forces at node j in the local directions *tnb* (3×1)
f_{tj}, f_{nj}, f_{bj}	external forces at node j in the local directions t, n, b respectively
$[m_{mj}]$	matrix of external moments at node j in the local directions *tnb* (3×1)
m_{tj}, m_{nj}, m_{bj}	external moments at node j in the local directions t, n, b respectively
$[F_{mj}]$	matrix of stress resultants / internal forces at node j in the local directions *tnb* (3×1)
F_{tj}, F_{nj}, F_{bj}	internal forces at node j in the local directions t, n, b respectively
$[M_{mj}]$	matrix of stress resultants / internal moments at node j in the local directions *tnb* (3×1)
M_{tj}, M_{nj}, M_{bj}	internal moments at node j in the local directions t, n, b respectively
$[C_{ij}]$	coordinate transformation matrix (3×3)
$[d\delta_{mj}]$	matrix of incremental finite displacements at node j in the local directions *tnb* (3×1)
$d\delta_{tj}$, $d\delta_{nj}$, $d\delta_{bj}$	incremental finite displacements at node j in the local directions t, n, b respectively
$[d\varphi_{mj}]$	matrix of incremental finite rotations at node j in the local directions *tnb* (3×1)
$d\varphi_{tj}$, $d\varphi_{nj}$, $d\varphi_{bj}$	incremental finite rotations at node j in the local directions t, n, b respectively
$[S_F]$, $[S_M]$	matrices of the elastic and geometrical properties (3×3)
E	modulus of elasticity
G	modulus of rigidity
ξ_n, ξ_b	shear coefficients about normal and binormal directions respectively
I_t	torsion constant
I_n, I_b	moment of inertia about normal and binormal directions respectively
$[d\delta_{sj}]$	matrix of incremental finite displacements at node j in the global directions *xyz* (3×1)
$d\delta_{xj}$, $d\delta_{yj}$, $d\delta_{zj}$	incremental finite displacements at node j in the global directions x, y, z

	respectively
$[d\varphi_{sj}]$	matrix of incremental finite rotations at node j in the global directions *xyz* (3×1)
$d\varphi_{xj}$, $d\varphi_{yj}$, $d\varphi_{zj}$	incremental finite rotations at node j in the global directions *x, y, z* respectively
$[d\delta_{sji}]$	matrix of transformed incremental finite displacements from node j to node i in the global directions *xyz* (3×1)
$d\delta_{xji}$, $d\delta_{yji}$, $d\delta_{zji}$	transformed incremental finite displacements from node j to node i in the global directions *x, y, z* respectively
$[d\varphi_{sji}]$	matrix of transformed incremental finite rotations from node j to node i in the global directions *xyz* (3×1)
$d\varphi_{xji}$, $d\varphi_{yji}$, $d\varphi_{zji}$	transformed incremental finite rotations from node j to node i in the global directions *x, y, z* respectively
$[\delta_{si}]$	matrix of total displacements at node i in the global directions *xyz* (3×1)
δ_{xi}, δ_{yi}, δ_{zi}	total displacements at node i in the global directions *x, y, z* respectively
$[\varphi_{si}]$	matrix of total rotations at node i in the global directions *xyz* (3×1)
φ_{xi}, φ_{yi}, φ_{zi}	total rotations at node i in the global directions *x, y, z* respectively
$[\delta_{mi}]$	matrix of total displacements at node i in the local directions *tnb* (3×1)
δ_{ti}, δ_{ni}, δ_{bi}	total displacements at node i in the local directions *t, n, b* respectively
$[\varphi_{mi}]$	matrix of total rotation at node i in the local directions *tnb* (3×1)
φ_{ti}, φ_{ni}, φ_{bi}	total rotation at node i in the local directions *t, n, b* respectively
$[Fm]_{00}$	flexibility matrix corresponding to node 0 in the loacal directions *tnb* (6×6)
$[Km]$	stiffness matrix in the local directions *tnb* (12×12)
$[Km]_{00}$, $[Km]_{0n}$, $[Km]_{n0}$, $[Km]_{nn}$	stiffness sub-matrices in the local directions *tnb* (6×6)
$[Ks]$	stiffness matrix in the global directions *xyz* (12×12)
$[Ks]_{00}$, $[Ks]_{0n}$, $[Ks]_{n0}$, $[Ks]_{nn}$	stiffness sub-matrices in the global directions *xyz* (6×6)
$[Tr]_{n0}$	transformation matrix corresponding to node n and node 0 (6×6)
$[R_T]_0$, $[R_T]_n$	rotation transformation matrix of the node 0 and node n respectively (6×6)
k11, k12, …, k69, …, (k12,12)	stiffness coefficients of stiffness matrix $[Km]$

Acknowledgement

We are thankful to Prof. Binita A. Vyas, Associate Professor, Applied Mechanics Department, Government Engineering College, Modasa, and Prof. Poonam I. Modi, Assistant Professor, Applied Mechanics, L. D. College of Engineering for proofreading this manuscript.

References

[1] S. N. Atluri, M. Iura, S. Vasudevan, A consistent theory of finite stretches and finite rotations, in space-curved beams of arbitrary cross-section, *Computational Mechanics,* Vol. 27, No. 4, pp. 271-281, 2001/04/01, 2001.

[2] A. Kaveh, K. Koohestani, N. Taghizadieh, Efficient finite element analysis by graph-theoretical force method, *Finite Elements in Analysis and Design - FINITE ELEM ANAL DESIGN,* Vol. 43, pp. 543-554, 04/01, 2007.

[3] A. Kaveh, K. Koohestani, Efficient finite element analysis by graph-theoretical force method; triangular and rectangular plate bending elements, *Finite Elements in Analysis and Design,* Vol. 44, No. 9, pp. 646-654, 2008/06/01/, 2008.

[4] A. Kaveh, M. Daei, Efficient force method for the analysis of finite element models comprising of triangular elements using ant colony optimization, *Finite Elements in Analysis and Design,* Vol. 45, No. 10, pp. 710-720, 2009/08/01/, 2009.

[5] A. Kaveh, E. N. Nasab, A new four-node quadrilateral plate bending element for highly sparse and banded flexibility matrices, *Acta Mechanica,* Vol. 209, No. 3, pp. 295-309, 2010/01/01, 2010.

[6] S. Patnaik, An integrated force method for discrete analysis, *International Journal for Numerical Methods in Engineering,* Vol. 6, No. 2, pp. 237-251, 1973.

[7] S. N. Patnaik, D. A. Hopkins, G. R. Halford, *Integrated force method solution to indeterminate structural mechanics problems,* pp. 2004.

[8] S. Ghuku, K. Saha, A Review on Stress and Deformation Analysis of Curved Beams under Large Deflection, *International Journal of Engineering and Technologies ISSN: 2297-623X,* Vol. 11, pp. 13-39, 07/13, 2017.

[9] K. Kang, J. Han, Analysis of a curved beam using classical and shear deformable beam theories, *KSME International Journal,* Vol. 12, pp. 244-256, 1998.

[10] T. Horibe, K. Mori, In-plane and Out-of-plane Deflection of J-shaped Beam, *Journal of Mechanical Engineering and Automation,* Vol. 5, No. 1, pp. 14-19, 2015.

[11] R. Palaninathan, P. S. Chandrasekharan, Curved beam element stiffness matrix formulation, *Computers & Structures,* Vol. 21, No. 4, pp. 663-669, 1985/01/01/, 1985.

[12] T. Dahlberg, Procedure to calculate deflections of curved beams, *International Journal of Engineering Education,* Vol. 20, pp. 503-513, 01/01, 2004.

[13] E. Marotta, P. Salvini, Analytical Stiffness Matrix for Curved Metal Wires, *Procedia Structural Integrity,* Vol. 8, pp. 43-55, 2018/01/01/, 2018.

[14] E. Tufekci, O. Y. Dogruer, Exact Solution of Out-of-Plane Problems of an Arch with Varying Curvature and Cross Section, *Journal of Engineering Mechanics-asce - J ENG MECH-ASCE,* Vol. 132, 06/01, 2006.

[15] F. N. Gimena, P. Gonzaga, L. Gimena, Analytical formulation and solution of arches defined in global coordinates, *Engineering Structures,* Vol. 60, pp. 189-198, 2014/02/01/, 2014.

[16] C. Dong, Structural Matrix Analysis of Variable Curvature Curved Beam, in *Proceeding of,* Atlantis Press, pp. 1727-1733.

[17] L. Gimena, F. N. Gimena, P. Gonzaga, Structural analysis of a curved beam element defined in global coordinates, *Engineering Structures,* Vol. 30, No. 11, pp. 3355-3364, 2008/11/01/, 2008.

[18] F. Gimena, P. Gonzaga, L. Gimena, Structural matrices of a curved-beam element, *Structural Engineering and Mechanics,* Vol. 33, 10/20, 2009.

[19] F. N. Gimena, P. Gonzaga, L. Gimena, 3D-curved beam element with varying cross-sectional area under generalized loads, *Engineering Structures,* Vol. 30, No. 2, pp. 404-411, 2008/02/01/, 2008.

[20] P. G. Lazaro Gimena, F. N. Gimena, Finite Transfer Method for the problem of spatially curved beams, in *Proceeding of.*

[21] F. Gimena, P. Gonzaga, L. Gimena, Stiffness and transfer matrices of a non-naturally curved 3D-beam element, *Engineering Structures - ENG STRUCT,* Vol. 30, pp. 1770-1781, 06/01, 2008.

[22] F. N. Gimena, P. Gonzaga, L. Gimena, Numerical transfer-method with boundary conditions for arbitrary curved beam elements, *Engineering Analysis with Boundary Elements,* Vol. 33, No. 2, pp. 249-257, 2009/02/01/, 2009.

[23] W. Bu, H. Xu, Curved beam elasticity theory based on the displacement function method using a finite difference scheme, *Advances in Difference Equations,* Vol. 2019, 04/15, 2019.

[24] C.-N. Chen, Out-of-plane deflection of nonprismatic curved beam structures solved by DQEM, *Advances in Engineering Software - AES,* Vol. 34, pp. 297-306, 05/01, 2003.

[25] G. Zhang, R. Alberdi, K. Khandelwal, Analysis of three-dimensional curved beams using isogeometric approach, *Engineering Structures,* Vol. 117, pp. 560-574, 06/01, 2016.

[26] M. Arici, M. Granata, Generalized curved beam on elastic foundation solved by Transfer Matrix Method, *Structural engineering & mechanics,* Vol. 40, pp. 279-295, 10/25, 2011.

[27] T. Yoda, H. Fuyama, M. Hirashima, VALIDITY OF AN ANALYSIS OF THIN-WALLED HELICOIDAL I-SECTION BEAMS APPROXIMATED BY AN ASSEMBLAGE OF STRAIGHT BEAMS, *Proceedings of the Japan Society of Civil Engineers,* Vol. 1983, No. 335, pp. 175-181, 1983.

[28] J. n. Murín, V. r. Kutiš, 3D-beam element with continuous variation of the cross-sectional area, *Computers & Structures,* Vol. 80, pp. 329-338, 02/01, 2002.

[29] F. Sarria, F. N. Gimena, P. Gonzaga, M. Goñi, L. Gimena, Formulation and Solution of Curved Beams with Elastic Supports, in *Proceeding of.*

[30] M. N. Fardis, A.-M. O. Skouteropoulou, S. N. Bousias, Stiffness matrix of free-standing helical stairs, *Journal of Structural Engineering,* Vol. 113, No. 1, pp. 74-87, 1987.

[31] S. Rajasekaran, S. Padmanabhan, Equations of curved beams, *Journal of engineering mechanics,* Vol. 115, No. 5, pp. 1094-1111, 1989.

[32] Y. Ai-min, Y. Ming, SOLUTION OF GENERALIZED COORDINATE FOR WARPING FOR NATURALLY CURVED AND TWISTED BEAMS, *Applied Mathematics and Mechanics (English Edition)*, Vol. 25, No. 10, pp. 1166-1175, 2004-10-18, 2004.

[33] A. M. Yu, X. G. Yang, G. H. Nie, Generalized coordinate for warping of naturally curved and twisted beams with general cross-sectional shapes, *International Journal of Solids and Structures*, Vol. 43, No. 10, pp. 2853-2867, 2006/05/01/, 2006.

[34] M. Rezaiee-Pajand, N. Rajabzadeh-Safaei, An Explicit Stiffness Matrix for Parabolic Beam Element, *Latin American Journal of Solids and Structures*, Vol. 13, pp. 1782-1801, 09/01, 2016.

[35] L. Liu, N. Lu, Variational formulations, instabilities and critical loadings of space curved beams, *International Journal of Solids and Structures*, Vol. 87, pp. 48-60, 2016/06/01/, 2016.

[36] W. Guo, T. Deng, M. Ding, J. Wang, L. Mi, X. Cheng, Matrix Displacement Method for Behavior Analysis of Curved Beam Considering Bending-torsion Coupling, *DEStech Transactions on Engineering and Technology Research*, 2017.

[37] M. Rezaiee-Pajand, N. Rajabzadeh-Safaei, A. R. Masoodi, An efficient mixed interpolated curved beam element for geometrically nonlinear analysis, *Applied Mathematical Modelling*, Vol. 76, pp. 252-273, 2019/12/01/, 2019.

[38] Y.-Q. Tang, E.-f. Du, J.-Q. Wang, J. Qi, A co-rotational curved beam element for geometrically nonlinear analysis of framed structures, *Structures*, Vol. 27, pp. 1202-1208, 10/01, 2020.

[39] A. Borković, B. Marussig, G. Radenković, Geometrically exact static isogeometric analysis of arbitrarily curved plane Bernoulli–Euler beam, *Thin-Walled Structures*, Vol. 170, pp. 108539, 2022.

[40] A. Borković, B. Marussig, G. Radenković, Geometrically exact static isogeometric analysis of an arbitrarily curved spatial Bernoulli–Euler beam, *Computer Methods in Applied Mechanics and Engineering*, Vol. 390, pp. 114447, 2022/02/15/, 2022.

[41] A. Al-Azzawi, 2008, *Numerical Analysis of Curved Thin Beams on Winkler Foundation*,

[42] A. Al-Azzawi, A. S. Shaker, Finite difference analysis of curved deep beams on Winkler foundation, *ARPN Journal of Engineering and Applied Sciences*, Vol. 6, pp. 42-48, 03/01, 2011.

[43] A. Cazzani, M. Malagu, E. Turco, Isogeometric analysis of plane curved beams, *Mathematics and Mechanics of Solids*, Vol. 21, 04/20, 2014.

[44] Y. He, X. Zhang, J. Geng, X. Chen, Z. Li, Two Kinds of Variables Finite Element Based on B-Spline Wavelet on Interval for Curved Beam, *International Journal of Applied Mechanics*, Vol. 11, 02/17, 2019.

[45] A. Pydah, A. Sabale, Static Analysis of Bi-directional Functionally Graded Curved Beams, *Composite Structures*, Vol. 160, 10/01, 2016.

[46] G. De Pietro, A. G. de Miguel, E. Carrera, G. Giunta, S. Belouettar, A. Pagani, Strong and weak form solutions of curved beams via Carrera's unified formulation, *Mechanics of Advanced Materials and Structures*, Vol. 27, pp. 1-12, 11/05, 2018.

[47] E. Marotta, L. Massimi, P. Salvini, Modelling of structures made of filiform beams: Development of a curved finite element for wires, *Finite Elements in Analysis and Design*, Vol. 170, pp. 103349, 11/01, 2019.

[48] M. Horák, E. La Malfa Ribolla, M. Jirásek, Efficient formulation of a two-noded geometrically exact curved beam element, *International Journal for Numerical Methods in Engineering*, Vol. 124, No. 3, pp. 570-619, 2023.

[49] M. Jirásek, E. La Malfa Ribolla, M. Horák, Efficient finite difference formulation of a geometrically nonlinear beam element, *International Journal for Numerical Methods in Engineering*, Vol. 122, No. 23, pp. 7013-7053, 2021.

[50] A. Cammarata, P. D. Maddio, R. Sinatra, N. P. Belfiore, Direct Kinetostatic Analysis of a Gripper with Curved Flexures, *Micromachines*, Vol. 13, No. 12, pp. 2172, 2022.

[51] G. Radenković, A. Borković, On the analytical approach to the linear analysis of an arbitrarily curved spatial Bernoulli–Euler beam, *Applied Mathematical Modelling*, Vol. 77, pp. 1603-1624, 2020/01/01/, 2020.

[52] C. Iandiorio, P. Salvini, Large displacements of slender beams in plane: Analytical solution by means of a new hypergeometric function, *International Journal of Solids and Structures*, Vol. 185-186, pp. 467-484, 2020/03/01/, 2020.

[53] D. Magisano, L. Leonetti, G. Garcea, Isogeometric analysis of 3D beams for arbitrarily large rotations: Locking-free and path-independent solution without displacement DOFs inside the patch, *Computer Methods in Applied Mechanics and Engineering*, Vol. 373, pp. 113437, 01/01, 2021.

[54] K. Wu, G. Zheng, G. Hao, Efficient Spatial Compliance Analysis of General Initially Curved Beams for Mechanism Synthesis and Optimization, *Mechanism and Machine Theory*, Vol. 162, 03/30, 2021.

[55] A. Amoozandeh, G. Radaelli, W. van de Sande, R. Ostayen, J. Herder, Characterization of spatially curved beams with anisotropically adaptive stiffness using sliding torsional stiffeners, *International Journal of Mechanical Sciences,* Vol. 234, pp. 107687, 08/01, 2022.

[56] R. Kapania, J. Li, A formulation and implementation of geometrically exact curved beam elements incorporating finite strains and finite rotations, *Computational Mechanics,* Vol. 30, No. 5, pp. 444-459, 2003.

[57] F. Kiarasi, M. Babaei, S. Mollaei, M. Mohammadi, K. Asemi, Free vibration analysis of FG porous joined truncated conical-cylindrical shell reinforced by graphene platelets, *Advances in nano research,* Vol. 11, No. 4, pp. 361, 2021.